Heat Loss Compensation for Semi-Adiabatic Calorimetric Tests

Peter Fjellström
M.Sc., Ph.D. Student
Luleå University of Technology
Dept. of Structural Engineering
SE - 97187 Luleå
peter.fjellstrom@ltu.se

Dr. Jan-Erik Jonasson
Professor
Luleå University of Technology
Dept. of Structural Engineering
SE – 97187 Luleå
jan-erik.jonasson@ltu.se

Dr. Mats Emborg
Head of R&D, Betongindustri AB
Professor, Head of Department
Luleå University of Technology
Dept. of Structural Engineering
SE – 97187 Luleå
mats.emborg@ltu.se

Dr. Hans Hedlund
Adj. Professor
Skanska Sverige AB
Technology
Bridge and Civil Engineering
SE – 405 18 Göteborg
hans.hedlund@skanska.se

ABSTRACT

Heat of hydration has long been of importance since it affects the temperature levels within a concrete structure, and thus, potentially affects its durability. The only source of energy is the reaction between cement and water. This energy warms up the concrete sample and all the ambient materials. Therefore, in order to model these energies, the TSA (traditional semi-adiabat) setup is transformed into an associated sphere. By this, the temperature distribution and the energies within each layer of the TSA can be calculated. The sum of all energies gives the total heat of hydration. A refined model using a correction factor is introduced, which accounts for energies lost to the TSA setup materials. Results show that the effect of this factor cannot be disregarded, especially not for TSAs with low cooling factors.

Key words: concrete, heat of hydration, adiabatic calorimetry, semi-adiabatic calorimetry, heat flow, correction factor, cooling factor.

1. INTRODUCTION

1.1 General

The energy quantity of the exothermic reaction between cement and water has long been of importance since it affects the temperature levels within a concrete structure, which can, based on risks of thermal cracking, affect the durability. The temperature influences the development of the pore structure in concrete [1, 2] and naturally its mechanical properties, e.g. strength [3]. For building engineering purposes heat of hydration has commonly been determined by various versions of adiabatic calorimeters, see Figure 1.

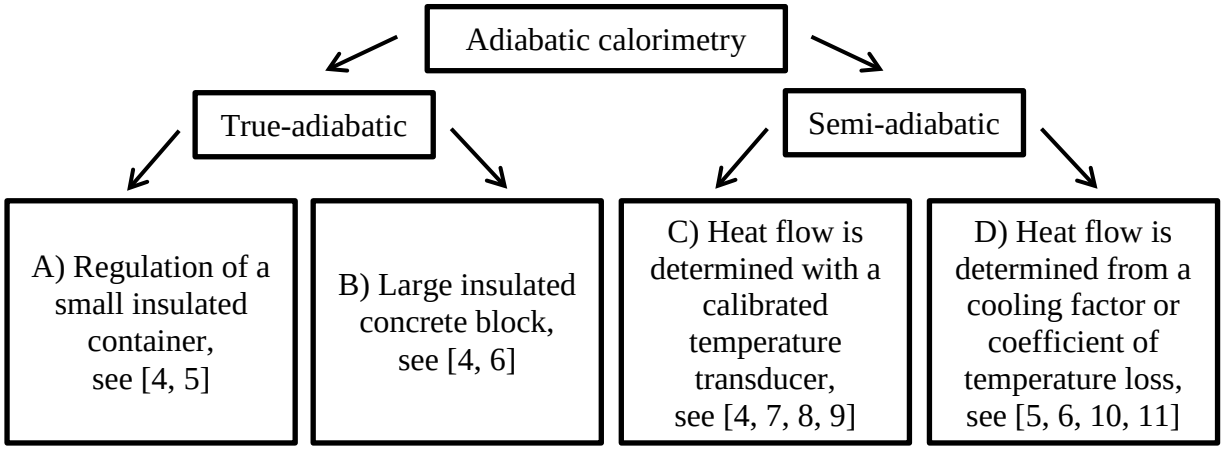

Figure 1 – Schematic presentation of adiabatic calorimetry.

In both the true-adiabatic and the semi-adiabatic setups the concrete temperature is registered as a function of time. The difference is that in the true-adiabatic setup no heat loss to the environment is supposed to be present. The semi-adiabatic setup allows for energy losses, which are accounted for in the evaluation process.

The true adiabatic measurement is in theory preferred, since it could give a correct value of heat of hydration direct from the test results. However, in A) it is hard to regulate the temperature, which can drift, and therefore the results are not always reliable [12]. In B) temperature measurement in the centre of a large concrete block is estimated to have true adiabatic temperature. However, in [6] they account for heat flow as in C) for better accuracy. In the semi-adiabatic methods, when heat flow is calculated from the temperature of the concrete sample, the following conditions have to be fulfilled

- The temperature in the concrete sample and the ambient air are equal when starting the semi-adiabatic measurement.
- The air temperature is constant during the test period.

To ensure these conditions limits are usually specified, e.g. the temperature of the fresh concrete mix should be within ±2°C of the calorimeter temperature [5], and the ambient temperature where the calorimeter is placed should be within the limit 20±1°C [5]. In [10] the laboratory, where the mixing of the constituents of the concrete occurs, the air temperature should be within 20±2°C. The room, where the test is conducted, have the corresponding limit 20±1°C, and the reference temperature should not differ more than ±0,5°C throughout the test [10].

When heat flow is directly measured with a calibrated temperature transducer, the points above are not that important. However, limits are still used, and in [7] the laboratory, where the test is conducted and where the mortar constituents are stored, the room temperature should be within 20±2°C. In this paper, heat flow is calculated from the sample temperature, and, our limits are the same as in [7].

1.2 Existing models and limitations

In order to determine the quantity of heat of hydration in a semi-adiabatic test, heat losses must be determined. In [11] a "traditional" semi-adiabatic (TSA) setup is presented, and the cooling factor were formally expressed as

$$a = \frac{\sum_i h_i \cdot A_i}{V_c \cdot c_c \cdot \rho_c} \tag{1}$$

Based on measured values of a [11] heat energy within the concrete sample, and heat losses based on heat flow, was expressed as

$$q_{cem} = \frac{\rho_c \cdot c_c}{C} \cdot \left(\left(T_c(t) - T_{air} \right) + a \cdot \int_0^t \left(T_c(t) - T_{air} \right) \cdot dt \right) \tag{2}$$

where a [1/s or 1/h] = cooling factor; h_i [W/m^2 °C] = heat transfer coefficient of the individual insulation material; A_i [m^2] = heat flow area of the individual insulation material; V_c [m^3] = volume of the concrete sample; c_c [J/kg °C] = heat capacity by weight of concrete; ρ_c [kg/m^3] = concrete density; q_{cem} [J/kg] = heat of hydration per kg of cement; C [kg/m^3] = cement content; $T_c(t)$ [°C] = concrete temperature; and T_{air} [°C] = air temperature.

When heat of hydration is determined by Eq. 2 the following conditions are usually stated.

- There should be small temperature gradients within the concrete sample. Then the average concrete temperature is easily measured and is representative when calculating energy stored in the concrete.
- A large temperature increase in the concrete sample is favourable, since the measured temperature hereby gives a reasonable picture of the energy involved.

The consequence of these conditions is that low values of the cooling factor or heat loss coefficients are needed. Recommended values are less than 100 J/h°C for the total heat loss coefficient in [5, 10] and for the cooling factor less than 0,035 h^{-1} in [13]. In [12] cooling factors between 0,020-0,025 h^{-1} are used, and lower values are recommended for reliable long term heat release measurements. However, when the amount of insulation is increased, more energy will be stored within the materials of the calorimetric setup during the test, and this is not accounted for by the traditional method using Eq. 2. For the thermos vessels in [5, 10] this is taken into account. However, these test setups are relatively complicated and expensive compared with TSAs. Therefore, this paper will focus on TSAs, and investigate the need of taking into account the energy stored within its relatively few parts.

2. AIMS AND PURPOSES

The TSA has the advantage that it can be built with inexpensive parts that are easily assembled. The temperature sensors are generally few, and the measurements can be performed quickly. The aims and purposes in this paper is to

- Demonstrate the existence and need of taking into account the energy that is heating up the equipment using a TSA.
- Develop a reasonable simple model for evaluation of the heat of hydration in concrete, which accounts for energy stored within the different parts of a TSA.
- Investigate how the different components of a TSA setup affect the amount of energy to be compensated for.

3. REFINED HEAT OF HYDRATION EVALUATION METHOD

3.1 Test preparation and procedure

First, concrete admixture proportions are determined in order to fulfil the specific recipes requirements, i.e. slump, air entrainment etc. Dry recipe constituents are mixed in the blender for 1 minute before adding water, and the total mixing time is 5 minutes. The concrete sample, of volume 4L is placed in a cylindrical metal bucket. The heating device, a Teflon carpet, is fixed around the bucket with a steel girdle and steel clamps. The mass of the sample is recorded before and after the semi-adiabatic test to ensure that no drying out has occurred. The concrete sample is put into the TSA about 15 minutes after mixing, and the temperature is recorded every 5 minute with sensors according to the numbers in Figure 2. In the square setup only sensors Nos. 1, 2 and 4 exist. Temperature sensors Nos. 1, 2 and 3 are placed in the concrete sample, and number 4 is located in the ambient air. In our laboratory, there exists two large (denoted A) and two small (denoted B) cylindrically shaped TSA, and three square (denoted C) TSAs.

The ambient air temperature in the laboratory varies very little and can be considered to be well within the range 20±2°C. Heat of hydration is measured until the concrete sample has approximately reached the temperature of the ambient air, which usually takes about 7 days. Then, without removing the concrete sample from the TSA, the concrete sample is heated to a level of maximum measured hydration temperature + 5°C. An empirical value of the cooling factor can then be determined by analysing the spontaneously cooling behaviour.

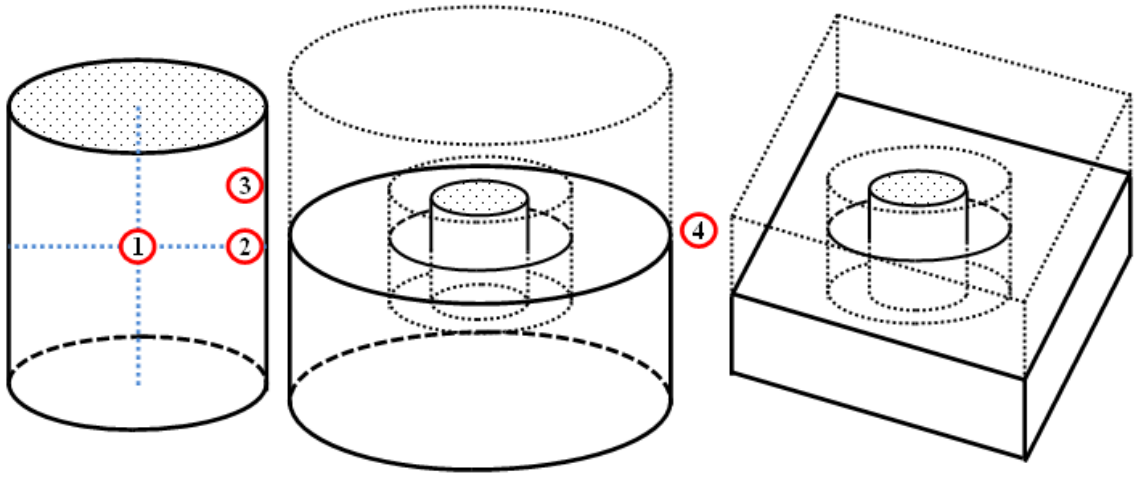

Figure 2 – Sample, cylindrical and square TSA units are shown in order from left to right. All TSAs use cellular plastic as insulation material. In addition, the square setup has an outer layer of plywood.

3.2 Empirical determination of the cooling factor

For a specific TSA setup with a constant volume of the concrete sample, the only variables should be the density and the thermal capacity of the concrete sample, see Eq. 1. However, other influencing factors may exist, e.g. aging of the TSA or some deviations in the placing of different components in the TSA setup. Therefore, to take possible variations into account, it is preferred to measure the cooling factor on each concrete sample before removing it from the test setup. A spontaneous cooling behaviour for a concrete sample is illustrated in Figure 3.

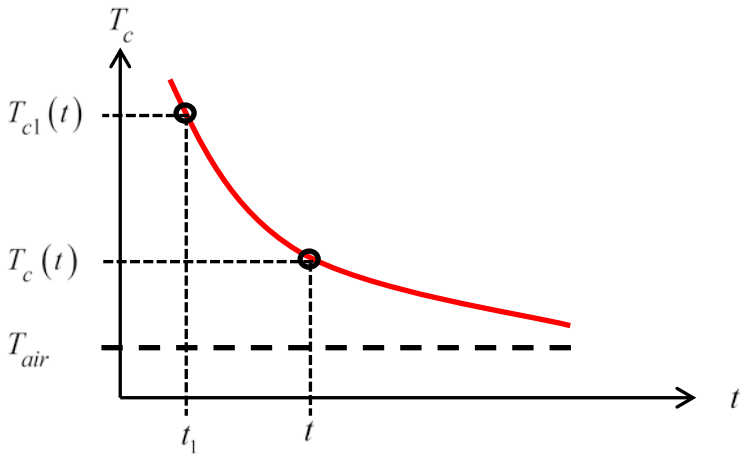

Figure 3 – Cooling behaviour for a mature concrete sample.

The common definition of the cooling factor is

$$\frac{dT}{dt} = a \cdot \left(T_c(t) - T_{air} \right) \tag{3}$$

Integrating this expression with the information given in Figure 3 results in Eq. 4, which can be fitted against empirical data with regression analysis. Here, the so called least square method is used.

$$a = \frac{\ln\left(\frac{T_c(t) - T_{air}}{T_{c1}(t) - T_{air}}\right)}{(t - t_1)} \tag{4}$$

where $T_c(t)$[°C] = temperature in the concrete sample at time t[s or h]; $T_{c1}(t)$[°C] = temperature in the concrete body at time t_1[s or h].

3.3 Evaluation and modelling of heat of hydration

From the TSA measurement the evaluated heat of hydration produced per kg of cement can be determined by summation for each time step of the energy stored within the concrete sample, within the TSA components, and the energy loss due to heat flow from the concrete sample to the surrounding air, expressed by

$$q_{cem} = \frac{\rho_c \cdot c_c}{C} \cdot \left[\eta \cdot \left(T_c(t) - T_{air}\right) + a \cdot \int_0^t \left(T_c(t) - T_{air}\right) \cdot dt \right] \tag{5}$$

where η[-] = correction factor introduced in this paper accounting for heat energy used to warm up the TSAs components.

It must be noted that the model in [5, 10] could have been formulated in this way in order to fit both a thermos vessel and a TSA. Therefore, the model in this paper has been designed to suit any semi-adiabatic setup.

For normal weight concrete an approximate linear relationship exists between the water/cement ratio (w/C) of the concrete mixture and its thermal capacity [14]. However, it is quite cumbersome to determine the “correct” thermal capacity from material point of view. We calculate energies from measured temperatures, and then, before application in calculations, translate these energies back to temperatures. This is a “mathematical recirculation”, which implies that information regarding concrete density and thermal capacity does not need to be known as “time” material properties. However, it is important to use the same values in the complete chain of methodology [15, 16], and acceptable constant values may be set to

$$\rho_c \cdot c_c = 2350 \cdot 1000 \,[\text{J/m}^3\text{°C}] \tag{6}$$

It has been shown that the heat of hydration is approximately proportional to the degree of hydration [17]. The formulation for the degree of hydration in [15] and [18] is modified and fitted against the empirical heat data expressed by

$$q_{cem} = q_u \cdot \alpha^* = q_u \cdot \exp\left(-\left[\ln\left(1 + \frac{t_e}{t_1} \right) \right]^{-\kappa_1} \right) \quad (7)$$

where α^* [-] = is the "relative" degree of hydration; t_1 [s or h], κ_1 [-] and q_u [J/kg] are fitting parameters determined by the so called least square method; t_e [s or h] = equivalent time. The notation relative means that $\alpha^* = 1$ reflects the ultimate heat of hydration, q_u, at the individual final value for a tested concrete.

It should be noted that the heat of hydration in Eq. 7 gives about the same results as the commonly used Danish TPM (three point model) formulation in [19] for the "decisive" part of the heat of hydration description. However, Eq. 7 is favourable for predictions outside the most decisive interval, specialty for more mature concrete [16], and, besides, Eq. 7 is zero when $t_e = 0$, which is preferable in programming.

4. DEVELOPED MODEL FOR THE CORRECTION FACTOR

4.1 General

In order to get a reasonable estimation of the generated heat in concrete, hydration heat flow to the environment and heat energy stored in the involved materials must be determined. Thus, temperature measurement from initiation of the test until the system is in equilibrium "in practice" with the ambient air temperature is needed. The following observations are of importance for the presented model

- The exothermic reaction between cement and water is the only source of energy.
- The reaction energy heats up the concrete body and the ambient materials.
- Heat flow in the surrounding insulation materials can be described by Fourier's Law of conductive heat transfer.

4.2 Prerequisites for the model for the correction factor

- The TSA unit can be transformed into an associated sphere, where the concrete volume is retained, and the measured cooling factor is reflected by the actual amount of insulation in the associated sphere.
- There is good thermal contact between the materials involved. In reality, there is a small amount, less than 5L, of air between the concrete sample and the cellular plastic for the TSAs in Figure 2. This air volume is assumed to be quickly warmed up to the same temperature as the concrete. The thermal capacity by weight of air is high and its density is low. Thus, its stored energy can be neglected in relation to the other involved materials, see Table 1. Calculations have shown that the energy stored in the air affects the correction factor by less than one thousandth for TSAs evaluated in this paper. Therefore, in the presented model using an associated sphere the first layer of insulation (cellular plastic) starts where the concrete ends.

Table 1 – Chosen values for the components involved in our TSA tests. Values within brackets are currently not needed for the model in this paper. In literature, these values may vary.

	Concrete	Steel	Teflon	Air	Cellular plastic	Plywood
k [W/m °C]	(2,1-1,7)	60	(0,25)	(0,026)	0,036	0,18
c [J/kg °C]	1000	450	1000	(1000)	1500	1700
ρ [kg/m^3]	2350	7850	(2150)	(1,2)	25	800

- The thermal conductivity in the concrete is significantly higher than in the surrounding insulation materials, see Table 1. Thus, if enough insulation material is used, it is reasonable to assume that there are no, or neglectable, temperature gradients within the concrete body. For our TSAs presented in Figure 2 laboratory measurements show that the maximum temperature difference from the centre of the sample to its surface is within the accuracy of the temperature sensors (±0,5°C).
- The temperature changes in the concrete sample are relatively slow. Therefore a stationary heat flow is assumed for the associated sphere, which significantly simplifies the temperature calculations in the insulation materials. To verify this claim, a cylindrical TSA that corresponds to the approximate average cooling factor observed during laboratory tests, $a = 0,028$ [1/h] was simulated in 2D with ConTeSt Pro [20]. The resulting non-stationary temperature profiles were then compared with stationary 2D calculations for a cylinder, see Figure 4. The stationary estimation is based on the average concrete temperature and follows the same procedure as the 3D stationary calculations presented in this paper for the associated sphere.

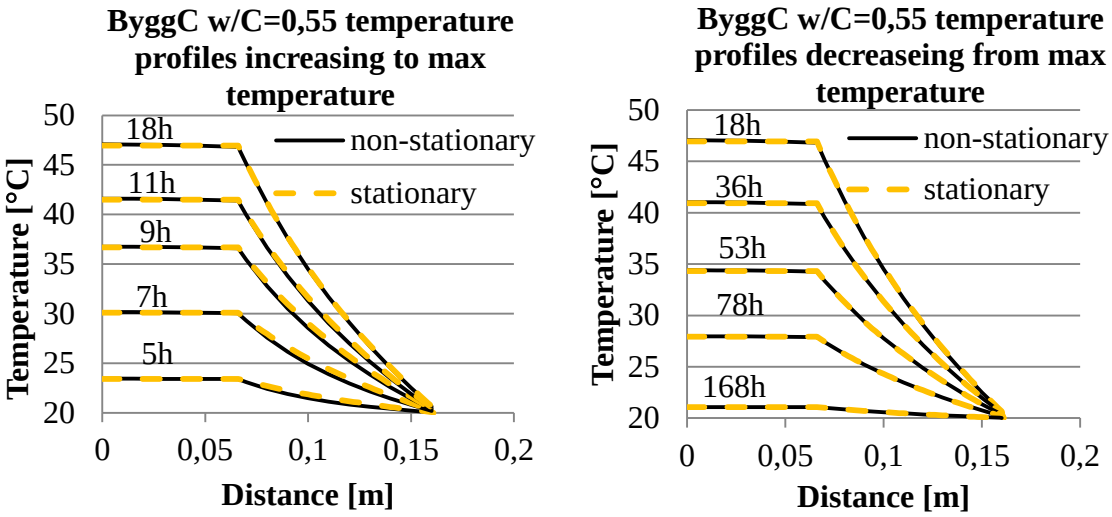

Figure 4 – Stationary and non-stationary temperature profiles in 2D simulations. The concrete radius r_c =0,066m and the insulation thickness is 0,094m. The chosen concrete mix is based on the "standard" cement used in this paper, see ByggC in Section 5.1.

A non-stationary behaviour can be observed for the hours that follow from start of the hydration process, where the stationary calculation shows a higher temperature within the insulation. This type of deviation increases for larger amount of insulation. The energy effect of this difference is illustrated by the correction factor for non-stationary and stationary conditions in Figure 5. Here, the correction factor is approximately equal after 10 hours. However, the consequences using a temporary "wrong" correction factor

during this “heat up” period is negligible in practice, as the total heat of hydration energy is very small in this period.

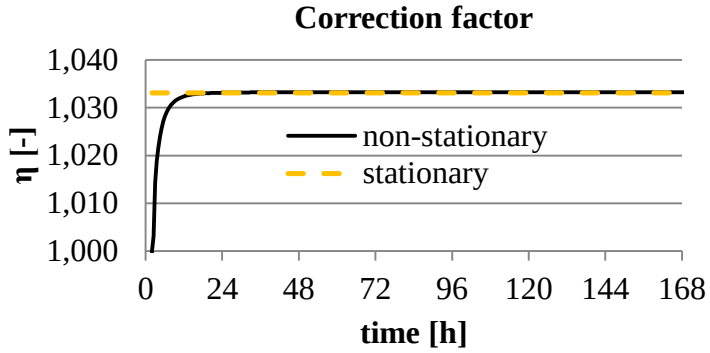

Figure 5 –The quotient between the energy stored within the insulation and the energy in the concrete when estimating the stationary and non-stationary correction factor.

4.3 Spherical heat transfer

In order to fit the model of an associated sphere to our laboratory setups, the concrete sample with radius r_c is surrounded by two materials, thicknesses l_{m1} and l_{m2}, see Figure 6.

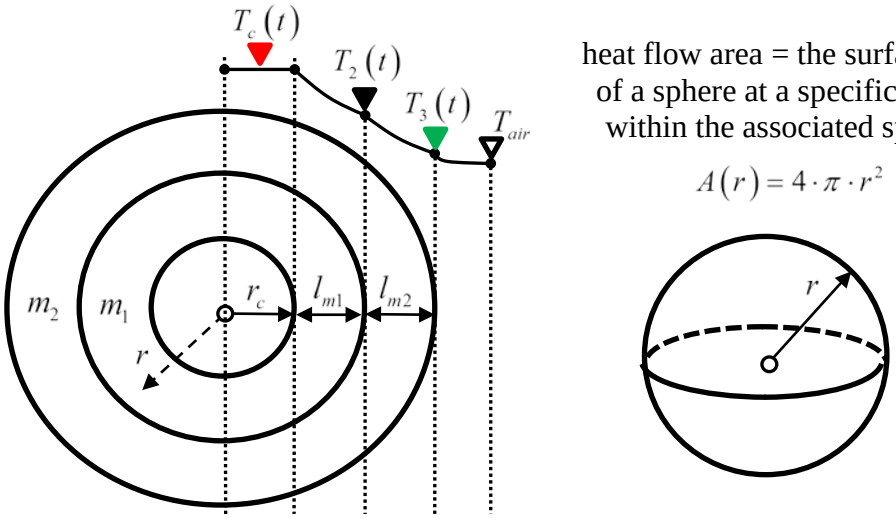

Figure 6 – A cross section of an associated sphere with a concrete sample surrounded by two layers of insulation materials. $A(r)$ [m^2] = heat flow area at any radius (r [m]).

Based on the information in Figure 6 the heat flow can be described by

$$\dot{Q}_{m1}(r,t) = -k_{m1} \cdot \frac{dT_{m1}(r,t)}{dr} \cdot 4 \cdot \pi \cdot r^2 \qquad \text{for} \qquad r_c \le r \le r_c + l_{m1} \tag{8}$$

$$\dot{Q}_{m2}(r,t) = -k_{m2} \cdot \frac{dT_{m2}(r,t)}{dr} \cdot 4 \cdot \pi \cdot r^2 \qquad \text{for} \quad r_c + l_{m1} \le r \le r_c + l_{m1} + l_{m2} \tag{9}$$

$$\dot{Q}_{air}(t) = h_{air} \cdot \left(T_3(t) - T_{air}\right) \cdot 4 \cdot \pi \cdot \left(r_c + l_{m1} + l_{m2}\right)^2 \quad \text{at} \quad r = r_c + l_{m1} + l_{m2} \tag{10}$$

$$\dot{Q}_{tot}(t) = h_{tot} \cdot \left(T_c(t) - T_{air}\right) \cdot 4 \cdot \pi \cdot r_c^2 \quad \text{at} \quad r = r_c \tag{11}$$

where $Q_i(r,t)$ [J] = energy in material i depending on time (t [s or h]) and radius (r [m]), and index i = m1 or m2; $\dot{Q}_i(r,t)$ [W] = $dQ_i(r,t)/dt$ = heat flow in material i; k_i [W/m °C] = thermal conductivity in material i; $T_i(r,t)$ [°C] = temperature in material i; l_i [m] = thickness of material i; $\dot{Q}_{air}(t)$ [W] = heat flow from the outer surface to air; h_{air} [W/m^2 °C] = heat transfer coefficient from the outer surface to air; T_3 [°C] = temperature at the outer surface; T_{air} [°C] = air temperature; $\dot{Q}_{tot}(t)$ [W] = heat flow from concrete to air; h_{tot} [W/m^2 °C] = heat transfer coefficient from concrete to air; $T_c(t)$ [°C] = temperature in the concrete body.

For a stationary heat flow Eqs. 8-11 describe the same flow formulated by

$$\dot{Q}_{m1}(r,t) = \dot{Q}_{m2}(r,t) = \dot{Q}_{air}(t) = \dot{Q}_{tot}(t) = \dot{Q}_{hf}(t) \tag{12}$$

where $\dot{Q}_{hf}(t)$ [W] = is the stationary heat flow at time t.

All equations concerning heat flow and temperature distribution in the subsequent text in this chapter are based on stationary heat flow conditions. In order to determine the temperature $T_{m1}(r,t)$ at specific point at time t within the material 1, the following integration needs to be performed

$$\frac{\dot{Q}_{hf}(t)}{k_{m1} \cdot 4 \cdot \pi} \cdot \int_r \frac{dr}{r^2} = \int_T -dT_{m1}(r,t) \tag{13}$$

if the boundary conditions are known it becomes

$$\frac{\dot{Q}_{hf}(t)}{k_{m1} \cdot 4 \cdot \pi} \cdot \int_{r_c}^{r} \frac{dr}{r^2} = -\int_{T_c(t)}^{T_{m1}(r,t)} dT_{m1}(r,t) \tag{14}$$

which gives

$$\frac{\dot{Q}_{hf}(t)}{k_{m1} \cdot 4 \cdot \pi} \cdot \left(\frac{1}{r_c} - \frac{1}{r}\right) = T_c(t) - T_{m1}(r,t) \tag{15}$$

The boundary temperature in the concrete sample, $T_c(t)$, can be measured at any time. Then, the temperature $T_{m1}(r,t)$ can be calculated for any point $r_c \le r \le r_c + l_{m1}$ at time t within the material 1 expressed by

$$T_{m1}(r,t) = T_c(t) - \frac{\dot{Q}_{hf}(t)}{k_{m1} \cdot 4 \cdot \pi} \cdot \left(\frac{r - r_c}{r_c \cdot r} \right) \tag{16}$$

At the end of material 1, where $r = r_c + l_{m1}$, we let $T_{m1}(r,t) = T_2(t)$, see Figure 6. Then, the corresponding expression for material 2 becomes

$$T_{m2}(r,t) = T_2(t) - \frac{\dot{Q}_{hf}(t)}{k_{m2} \cdot 4 \cdot \pi} \cdot \left(\frac{r - (r_c + l_{m1})}{(r_c + l_{m1}) \cdot r} \right) \tag{17}$$

At the end of material 2, where $r = r_c + l_{m1} + l_{m2}$, we let $T_{m2}(r,t) = T_3(t)$, see Figure 6.

Now, when the boundary conditions are known, T_2 and T_3 from Eqs. 16-17, by use of Eqs. 8-12 the temperature difference within each material is expressed as

$$T_c(t) - T_2(t) = \frac{\dot{Q}_{hf}(t) \cdot l_{m1}}{4 \cdot \pi \cdot k_{m1} \cdot r_c \cdot (r_c + l_{m1})} \tag{18}$$

$$T_2(t) - T_3(t) = \frac{\dot{Q}_{hf}(t) \cdot l_{m2}}{4 \cdot \pi \cdot k_{m2} \cdot (r_c + l_{m1}) \cdot (r_c + l_{m1} + l_{m2})} \tag{19}$$

$$T_3(t) - T_{air} = \frac{\dot{Q}_{hf}(t)}{h_{air} \cdot 4 \cdot \pi \cdot (r_c + l_{m1} + l_{m2})^2} \tag{20}$$

$$T_c(t) - T_{air} = \frac{\dot{Q}_{hf}(t)}{h_{tot} \cdot 4 \cdot \pi \cdot r_c^2} \tag{21}$$

Summation of the temperature differences from the concrete sample to the air gives

$$T_c(t) - T_{air} = (T_c(t) - T_2(t)) + (T_2(t) - T_3(t)) + (T_3(t) - T_{air}) \tag{22}$$

Substituting Eqs. 18-21 into Eq. 22 gives the total heat transfer coefficient from the concrete sample to the air expressed by

$$h_{tot} = \frac{1}{r_c^2} \cdot \left(\frac{l_{m1}}{k_{m1} \cdot r_c \cdot (r_c + l_{m1})} + \frac{l_{m2}}{k_{m2} \cdot (r_c + l_{m1}) \cdot (r_c + l_{m1} + l_{m2})} + \frac{1}{h_{air} \cdot (r_c + l_{m1} + l_{m2})^2} \right)^{-1} \tag{23}$$

Thus, the individual temperatures within each material, Eqs. 18-21, can be determined by the heat flow expression in Eq. 11.

4.4 Heat energy stored within the materials of the TSA

In order to account for the amount of energy heating up material 1 of the TSA, the average temperature within the material, T_{m1}^{ave}, is expressed as

$$T_{m1}^{ave} = \frac{1}{V_{m1}} \cdot \int_{r_c}^{r_c+l_{m1}} T_{m1}(r,t) \cdot 4 \cdot \pi \cdot r^2 \cdot dr \tag{24}$$

where $V_{m1}\,[\mathrm{m}^3] = \frac{4 \cdot \pi}{3} \cdot \left[(r_c + l_{m1})^3 - r_c^3 \right]$ is the volume for material 1, which gives

$$T_{m1}^{ave}(t) = \frac{3}{(r_c + l_{m1})^3 - r_c^3} \cdot \left\{ \begin{array}{l} \left(T_c(t) - \frac{h_{tot} \cdot (T_c(t) - T_{air}) \cdot r_c}{k_{m1}} \right) \cdot \left[\frac{(r_c + l_{m1})^3 - r_c^3}{3} \right] \\ + \frac{h_{tot} \cdot (T_c(t) - T_{air}) \cdot r_c^2}{k_{m1}} \cdot \left[\frac{(r_c + l_{m1})^2 - r_c^2}{2} \right] \end{array} \right\} \tag{25}$$

The corresponding expression for the average temperature in material 2, T_{m2}^{ave}, is expressed by

$$\begin{array}{l} T_{m2}^{ave}(t) = \frac{3}{(r_c + l_{m1} + l_{m2})^3 - (r_c + l_{m1})^3} \cdot \\ \left\{ \begin{array}{l} \left(T_2(t) - \frac{h_{tot} \cdot (T_c(t) - T_{air}) \cdot r_c^2 \cdot (r_c + l_{m1})}{k_{m2}} \right) \cdot \left[\frac{(r_c + l_{m1} + l_{m2})^3 - (r_c + l_{m1})^3}{3} \right] + \\ \frac{h_{tot} \cdot (T_c(t) - T_{air}) \cdot r_c^2}{k_{m2}} \cdot \left[\frac{(r_c + l_{m1} + l_{m2})^2 - (r_c + l_{m1})^2}{2} \right] \end{array} \right\} \end{array} \tag{26}$$

Thus, the thermal energy in each of the materials are expressed as

Concrete $$Q_c(t) = \rho_c \cdot c_c \cdot V_c \cdot (T_c(t) - T_{air}) \tag{27}$$

Material 0 $$Q_{m0}(t) = \sum_j (\rho_j \cdot c_j \cdot V_j) \cdot (T_c(t) - T_{air}) \tag{28}$$

Material 1 $$Q_{m1}(t) = \rho_{m1} \cdot c_{m1} \cdot V_{m1} \cdot (T_{m1}^{ave}(t) - T_{air}) \tag{29}$$

Material 2 $$Q_{m2}(t) = \rho_{m2} \cdot c_{m2} \cdot V_{m2} \cdot (T_{m2}^{ave}(t) - T_{air}) \tag{30}$$

where $m0$ = material 0 reflects the stored thermal energy for materials in direct contact with the concrete sample, which are considered to have the same temperature as the concrete sample; j = index for individual materials within material 0. In the TSA setup presented here, material 0

consists of a steel bucket ($j=1$), a steel girdle ($j=2$), steel clamps ($j=3$) and a heating carpet of Teflon ($j=4$).

The heat of hydration energy stored within material 0, material 1 and material 2 are all proportional to the heat of hydration energy stored in the concrete sample. Therefore the energy correction factor is expressed by

$$\eta(t)=1+\frac{Q_{m0}(t)+Q_{m1}(t)+Q_{m2}(t)}{Q_c(t)} \tag{31}$$

Eq. 31 formally describes the correction factor as a function of time. However, the energy in each material is proportional to the energy stored in the concrete sample reflected by the term $\left(T_c(t)-T_{air}\right)$. Therefore, the correction factor is constant and can be evaluated for any time t.

In Figure 7 the total heat of hydration energy at any time t is the sum of the energy stored in the materials of the TSA, i.e. the sum of Eqs. 27-30, and the energy loss from the TSA due to the accumulated heat flow, see the second part of Eq. 2. Based on a measured value of the cooling factor, a in Eq. 4, the energy due to heat flow, $Q_{hf}(t)$, is expressed by

$$Q_{hf}(t)=\int_0^t \dot{Q}_{hf}(t)\cdot dt=\rho_c\cdot c_c\cdot V_c\cdot a\cdot\int_0^t\left(T_c(t)-T_{air}\right)\cdot dt \tag{32}$$

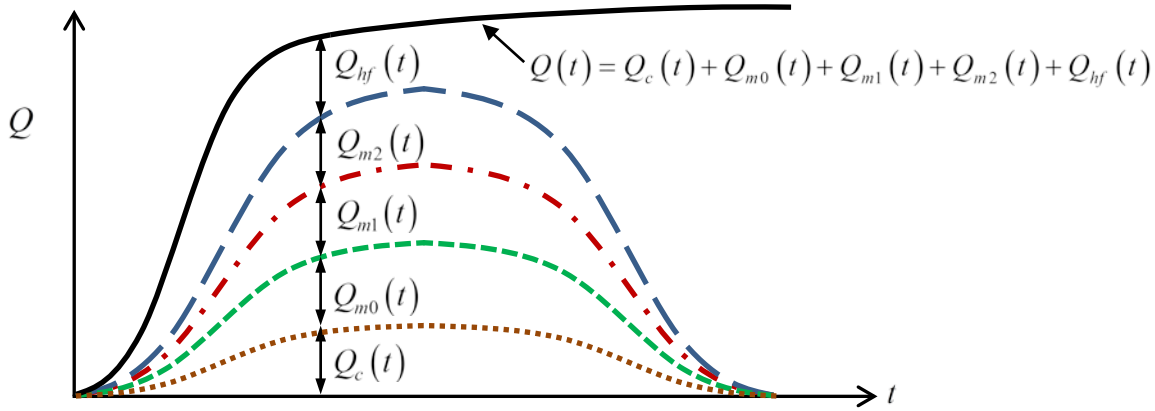

Figure 7 – The total energy is the sum of the energies stored in the concrete, the ambient materials and the energy loss to the surrounding air, see Eqs. 27-30 and 32. Note that this figure only illustrates the energies involved without respect to real size relations.

4.5 Determination of stationary heat transfer coefficient

In order to calculate the associated stationary temperature distribution the total heat transfer coefficient, h_{tot}, has to be calculated. The stationary heat flow based on the rate of temperature changes in the concrete sample is expressed by

$$\dot{Q}_{hf}(t)=\frac{dT_c(t)}{dt}\cdot V_c\cdot\rho_c\cdot c_c \tag{33}$$

Combining Eq. 11 with Eqs. 3 and 33 gives

$$h_{tot} \cdot \left(T_c\left(t\right) - T_{air}\right) \cdot 4 \cdot \pi \cdot r_c^2 = a \cdot \left(T_c\left(t\right) - T_{air}\right) \cdot \frac{4 \cdot \pi \cdot r_c^3}{3} \cdot \rho_c \cdot c_c \tag{34}$$

which results in

$$h_{tot} = \frac{a \cdot r_c \cdot \rho_c \cdot c_c}{3} \tag{35}$$

Eq. 35 expresses the parameter h_{tot} for an associated sphere with the same cooling factor as the real TSA.

4.6 Steps to determine the correction factor

1. Determine, or use Eq. 6, concrete density and heat capacity by weight. The volume of the concrete sample is known and is transformed into the associated concrete sphere with radius r_c. Heat capacity by weight for all materials in the TSA is also needed.

2. Determine, using data sheets or calibration, the thermal conductivity of all material layers, k_i, in the associated sphere.

3. The heat transfer coefficient from outer surface to air should be estimated. For our laboratory conditions h_{air} is approximately set to 10 W/m^2 °C.

4. Evaluate a cooling factor from the laboratory tests and calculate the total heat transfer coefficient, h_{tot} using Eq. 35.

5. The total heat transfer coefficient, h_{tot} in Eq. 35, reflects the real cooling factor. By using Eq. 23 and an iteration technique l_{m1} and l_{m2} can be determined. In cases with only one insulation material ($l_{m1} > 0$ and $l_{m2} = 0$) the use of Eq. 23 is straightforward. This is the case here for two cylindrical TSAs, see Figure 2.

6. The square TSA used here, see Figure 2, has an outer layer of plywood. The associated sphere is constructed with the condition that the relation between the stored energy per temperature unit is maintained between the two materials, which is expressed by

$$\delta_{m1,m2} = \frac{\rho_{m1} \cdot c_{m1} \cdot V_1}{\rho_{m2} \cdot c_{m2} \cdot V_2} \tag{36}$$

which gives

$$V_2 = \frac{1}{\delta_{m1,m2}} \cdot \frac{\rho_{m1} \cdot c_{m1} \cdot V_1}{\rho_{m2} \cdot c_{m2}} \tag{37}$$

where V_1 and V_2 are the real volumes of material 1 and material 2, respectively.

The volume of material 1 in the associated sphere is given by

$$V_{m1} = \frac{4 \cdot \pi}{3} \cdot \left[\left(r_c + l_{m1} \right)^3 - r_c^3 \right] \tag{38}$$

and the volume of material 2 in the associated sphere using Eq. 37 results in

$$V_{m2} = \frac{1}{\delta_{m1,m2}} \cdot \frac{\rho_{m1} \cdot c_{m1} \cdot V_{m1}}{\rho_{m2} \cdot c_{m2}} \tag{39}$$

and

$$V_{m2} = \frac{4 \cdot \pi}{3} \left[\left(r_c + l_{m1} + l_{m2} \right)^3 - \left(r_c + l_{m1} \right)^3 \right] \tag{40}$$

which gives

$$l_{m2} = \left[\frac{3 \cdot V_{m2}}{4 \cdot \pi} + \left(r_c + l_{m1} \right)^3 \right]^{1/3} - r_c - l_{m1} \tag{41}$$

7. The consequences of Eqs. 36-41 are that l_{m2} and V_{m2} are expressed as functions of l_{m1}. So, h_{tot} in Eq. 23 is solely a function of l_{m1}, and the size of l_{m1} is here determined by an iterative technique. l_{m2} is calculated using Eq. 41, and the size of the associated sphere is established. Now, the constant correction factor, Eq. 31, is determined for time t, see Figure 7.

5. EVALUATION OF THE EFFECT OF THE CORRECTION FACTOR

5.1 Tested concrete recipes

Here the purpose is to show how the correction factor affects the actual temperatures in a concrete structure. Two common Swedish cements are used, see Tables 2 and 3. AnlC is a "moderate heat" cement, that generally is used for civil engineering structures. ByggC is a "standard" cement causing higher concrete temperature than AnlC, and its application area is usually concerning housing.

Table 2 – Oxides, clinker minerals and specific surface of tested cements. ByggC is of type CEM II/A-LL 42,5 R containing about 13% LL, and AnlC is of type CEM I 42,5 N SR3 MH/LA produced by CEMENTA AB.

Cement	Oxides [%]					Clinker minerals [%]				Specific surface
	CaO	SiO_2	Al_2O_3	Fe_2O_3	SO_3	C_3S	C_2S	C_3A	C_4AF	[m^2/kg]
ByggC	61,4	18,7	3,9	2,8	3,5	54,1	8,9	5,1	7,8	460
AnlC	64,1	22,4	3,7	4,5	2,4	48,0	28,0	2,1	13,8	316

Table 3 – Main constituents of tested concretes.

Recipe	Cement	Cement content [kg/m^3]	w/C [-]
1	ByggC	360	0,55
2	AnlC	340	0,55

5.2 Calculated values of the correction factor

The materials in direct connection with the concrete sample in the TSAs are weighted in order to determine their stored energy, see Table 1 and 4.

Table 4 –Weighted components in direct connection with the concrete sample. The weight of the steel bucket includes the weight of a steel lid.

	Steel bucket [kg]	Steel clamps [kg]	Steel girdle [kg]	Teflon carpet [kg]
TSA A and B	0,427	0,164	0,069	0,099
TSA C	0,465			0,408

The heat of hydration for the recipes in Table 3 was evaluated from measurements performed in TSA A and B. The cooling factors and other parameters needed for the iteration process and their resulting correction factors are presented in Table 5.

Table 5 – Parameters used in the iteration process, and the resulting correction factor.

Recipe/ TSA	a [1/h]	h_{tot} [W / m^2°C]	h_{air} [W / m^2°C]	k_{m1} [W / m°C]	r_c [m]	l_{m1} [m]	V_{m1} [m^3]	η [-]
1/A	0,0237	0,5071	10	0,036	0,0985	0,2508	0,174	1,157
1/B	0,0327	0,7014	10	0,036	0,0985	0,1035	0,031	1,078
2/A	0,0259	0,5552	10	0,036	0,0985	0,1862	0,093	1,118
2/B	0,0324	0,6933	10	0,036	0,0985	0,1062	0,032	1,079

In the associated sphere the radius depends on the thickness of the concrete sample and the insulation, see Figure 6. A small decrease of the cooling factor gives a small increase of insulation thickness in material 1 (l_{m1}). However, the volume is significantly greater since it is a cubic function, see Eq. 38. Therefore, a small difference in cooling factor (a) for TSA A between recipe 1 and 2 in Table 5 results in a quite large difference in calculated volume (V_{m1}). The difference in energy stored within these insulation volumes are reflected by the correction factor in Table 5.

5.3 Evaluated heat of hydration

Both the traditional method, Eq. 2, and the refined method, Eq. 5, were used to evaluate heat of hydration (q_{cem}) for recipes 1 and 2 in Table 3. The parameters of Eq. 7 were fitted against the test results in Figure 8 from TSA A and B for each recipe, see Table 6.

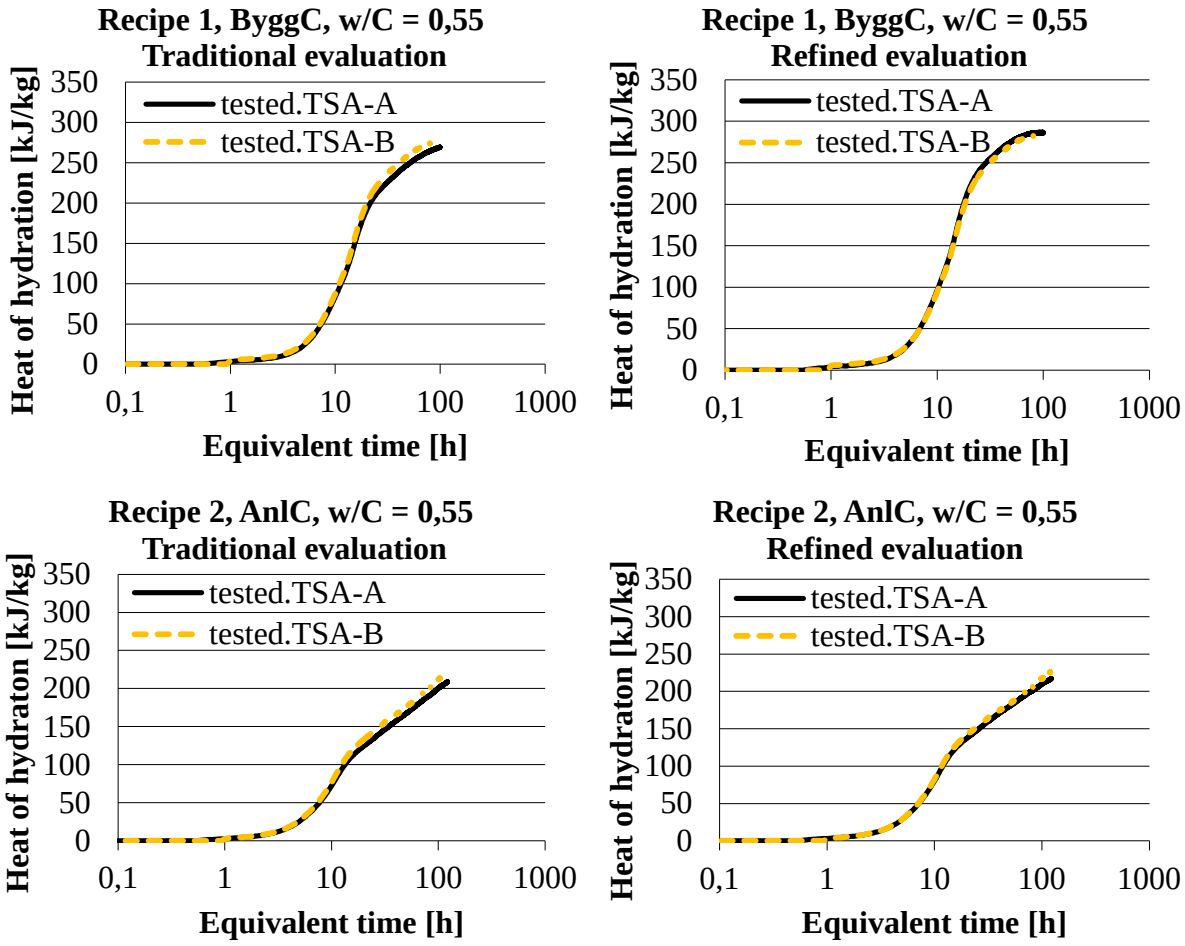

Figure 8 – Evaluated heat of hydration using the traditional method, Eq. 2, and the refined method, Eq. 5. Fitting parameters using Eq. 7 are presented in Table 6.

TSA A has a considerable lower value of the cooling factor compared to TSA B, see Table 5. This is caused by a higher amount of insulation material in TSA A. The energy stored in the insulation is reflected by the correction factor, which always is increased with decreased cooling factor. The consequence of not taking this energy into account using a larger TSA will result in a lower heat of hydration compared to a smaller TSA. This effect can be seen for the traditional evaluation in Figure 8 using the traditional evaluation, where TSA B is higher than TSA A. These results show that general recommendations concerning low cooling factors may result in too low heat of hydration using TSAs that are evaluated with the traditional method.

By using the refined evaluation the heat of hydration curves become approximately equal for the decisive part of the curves, see approximately equivalent time up to 100h in Figure 8. These results show that it is important to consider energies stored within the TSA materials.

Table 6 – Model parameters for evaluated heat of hydration results, see Eq. 7.

Recipe/TSA	Traditional evaluation (Eqs. 2 and 6)			Refined evaluation (Eqs. 5 and 6)		
	q_u [J/kg]	t_1 [h]	κ_1 [-]	q_u [J/kg]	t_1 [h]	κ_1 [-]
1/A	296000	6,54	2,28	300000	5,91	2, 27
1/B	309000	6,50	2,34	300000	6,23	2,96
2/A	420000	21,83	0,58	345000	11,01	0,85
2/B	358000	12,61	0,79	345000	10,39	0,87

5.4 Simulation of temperature development within walls

In order to determine the effect of the correction factor, the maximum temperature reached within a concrete structure was determined using the parameters in Table 6. This simulation was performed with ConTeSt Pro in 2D [20], where five concrete walls of different thicknesses with a formwork of plywood were studied. The air temperature was kept constant at 20°C, and the heat transfer coefficient from the outer surface to air (h_{air}) is set to 10 W/m^2 °C. The results are presented in Table 7 and 8

where ΔT_A and ΔT_B show the temperature difference between traditional and refined evaluation for TSA A and B, respectively; ΔT_{ABR} shows the temperature difference between the refined evaluation using TSA A and B.

Table 7 – Maximum temperature reached within a wall of different sizes, based on recipe 1.

Wall thickness [m]	Calculated temperatures, recipe 1, ByggC [°C]						
	1/A			1/B			1/(A+B)
	Traditional evaluation	Refined evaluation	ΔT_A	Traditional evaluation	Refined evaluation	ΔT_B	ΔT_{ABR}
0,1	36,6	40,7	-4,1	37,0	38,9	-1,9	1,8
0,2	42,9	47,4	-4,5	43,6	45,7	-2,1	1,7
0,4	49,3	53,6	-4,3	50,3	52,2	-1,9	1,4
0,8	55,3	58,9	-3,6	56,7	58,2	-1,6	0,7
1,6	60,0	62,4	-2,4	61,7	62,6	-0,9	-0,2

Table 8 – Maximum temperature reached within a wall of different sizes, based on recipe 2.

Wall thickness [m]	Calculated temperatures, recipe 2, AnlC [°C]						
	2/A			2/B			2/(A+B)
	Traditional evaluation	Refined evaluation	ΔT_A	Traditional evaluation	Refined evaluation	ΔT_B	ΔT_{ABR}
0,1	27,9	29,1	-1,2	28,9	29,7	-0,8	-0,6
0,2	31,7	33,2	-1,5	32,9	33,9	-1,0	-0,7
0,4	36,4	38,0	-1,6	37,7	38,8	-1,1	-0,8
0,8	41,8	43,4	-1,5	43,1	44,1	-1,0	-0,7
1,6	47,8	48,9	-1,1	48,7	49,4	-0,8	-0,5

The general behaviour for both ByggC and AnlC in Tables 7 and 8 are

- The maximum temperature level is higher for thicker walls for both traditional and refined evaluation.
- Traditional heat of hydration evaluation for TSA B gives a higher maximum temperature compared with TSA A, since less energy is lost to the smaller insulation material in TSA B.
- The temperature level is always higher for the refined evaluation compared to the traditional evaluation, since the energy in the surrounding materials are considered.
- ByggC is the “standard” cement with significantly higher heat of hydration during the decisive period and shows a higher maximum temperature compared to AnlC.
- ByggC shows a larger temperature difference between TSA A and B compared to AnlC, which is a consequence of that ByggC is the “faster” cement.
- The differences in ΔT_{ABR} are smallest for the refined evaluation and the largest wall. This indicates that the refined evaluation reflects the “true” material parameters, as the centre point of the thickest wall is most dependent on the heat of hydration.

The deviation of maximum temperatures between the traditional and the refined evaluation are of importance both for strength growth and crack risk calculations. For the larger TSA A and the faster cement ByggC the maximum difference in temperature is within 4,5°C, which for the estimation of strength growth can be regarded on “the safe side”, i.e. too low strength values and too long hardening times are calculated, but this “extra margin” might not be wanted in practice. For the calculation of crack risks, and especially for risks of through cracking at high restraint, 4,5°C underestimates the crack risk substantially. This is explained by the maximum addition of the design strain ratio [= additional tensile strain/failure tensile strain] might be as big as 0,7·4,5/10 = 0,32 [21, 22]. Let us assume that the design strain ratio is calculated to be at most 0,7 (rather common requirement for civil engineering structures), the “true” strain ratio will be 0,7 + 0,32 = 1,02. A strain ratio > 1 means obvious risk of cracking. Even a small temperature difference of about 2°C might result in an underestimation of the strain ratio with 0,14, which also is a too large difference in the calculations (0,7+0,14=0,84). Even if the underestimation in calculated strain ratios does not result in cracking, the margin in the safety factors are significantly reduced. Therefore, these results show that it is important to consider energies stored within the TSA materials.

5.5 Pre-calculated correction factors for TSAs at Luleå University of Technology

It has been shown that the correction factor will change due to the amount of insulation material in the TSA. For our cylindrical and square TSAs a normal span of cooling factors is between 0,023-0,034 1/h and 0,040-0,045 1/h, respectively. Therefore, an extended span with pre-calculated correction factors for corresponding cooling factors will simplify future evaluations, see Figures 9 and 10. In addition, a reasonable interval for normal weight concretes and their effect on the correction factor is shown. The thermal capacity by weight is kept constant at 1000 J/kg °C since it is cumbersome to establish in hydrating concrete.

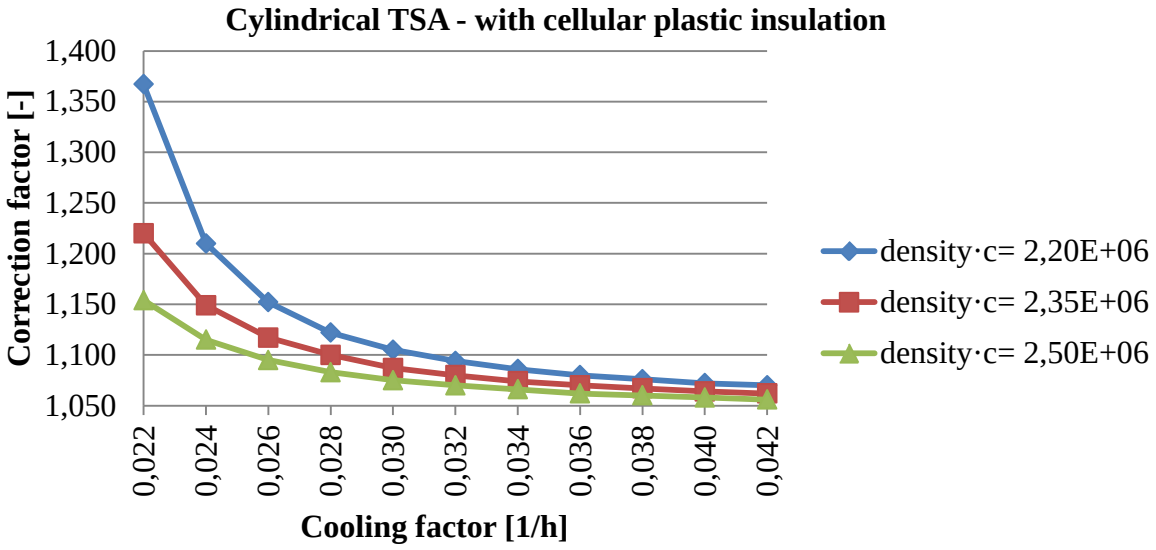

Figure 9 – Cooling and correction factor concerning TSA A and B.

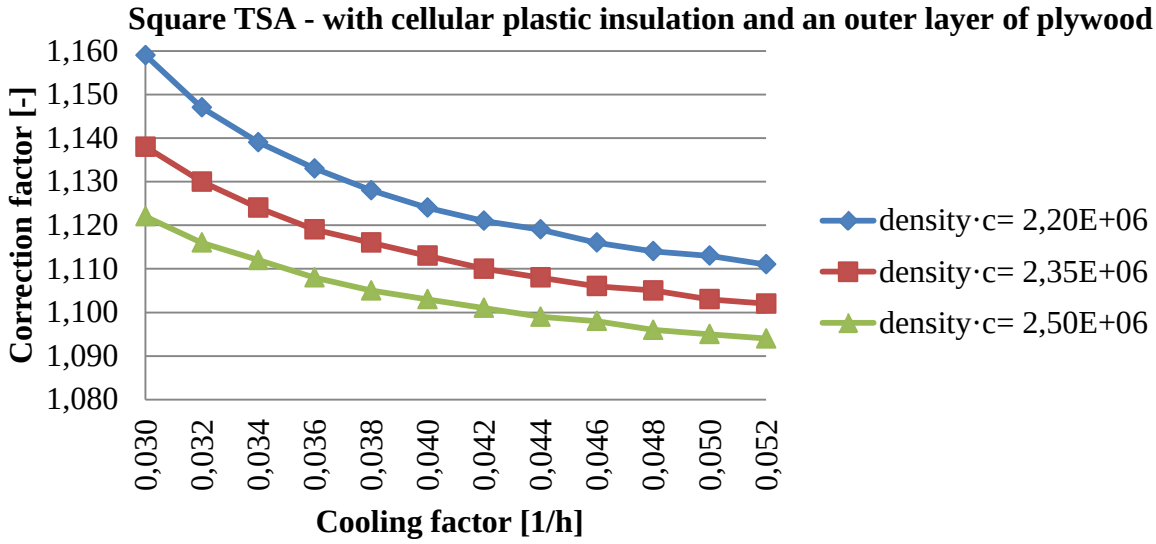

Figure 10 – Cooling and correction factor concerning TSA C.

In Figure 9 and 10 it can be seen that the higher the density, the lower cooling and correction factor. An increased amount of insulation gives a lower cooling factor, but a higher correction factor. Thus, it is again shown, that recommendations regarding low values of the cooling factor may result in too low hydration energy when evaluation is performed with the traditional method, Eq. 2.

6. SUMMARY AND CONCLUSIONS

The energy quantity of the exothermic reaction between cement and water has long been of importance since it affects the temperature levels within a concrete structure. Several adiabatic methods have been used to determine heat of hydration. The traditional semi-adiabat (TSA) has been popular to use for engineering purposes because of its simple construction with cheap parts.

The traditional evaluation method was presented in 1954 [11] and is still used today. Improvements to this evaluation method are found in [5] and [10], where energy stored in the semi-adiabatic setup is accounted for. However, the evaluation method in [5] and [10] only works for their specific semi-adiabatic setup using thermos vessels, and not for TSAs. Therefore, this paper presents a refined and general model that accounts for energies stored in the concrete sample and within all its surrounding materials, which is reflected by a correction factor formally increasing the energy in the concrete sample.

The concrete sample and the TSA are transformed into an associated sphere. The volume of the concrete sample is maintained in the associated sphere as the real volume in the TSA. The relative volume of the additional TSA materials within the associated sphere is determined by an iterative process, with the condition that the measured cooling factor is the same in the sphere. This paper presents a technique in which the only iterated parameter is the thickness of the first layer of insulation. Heat of hydration energy is calculated as the sum of energies in the concrete sample and all the surrounding materials. The correction factor reflects these additional energies in the surrounding materials. For our laboratory additional materials consist of a steel bucket, a

steel girdle, steel clamps, a heating carpet of Teflon and two layers of insulation. All these additional materials have a significant effect on the correction factor.

Two common Swedish cements are studied in this paper. ByggC is a “standard” cement and its application area is usually housing, and AnlC is a “moderate heat” cement generally used for civil engineering structures. The results from the heat of hydration evaluation using these concrete mixes show that TSA A has a considerable lower value of the cooling factor compared to TSA B. This is caused by the higher amount of insulation material in TSA A, as TSAs with lower cooling factors always store more energy in the surrounding material for a specific mix. Without compensation for this additional energy in the evaluation process, a lower cooling factor always results in a lower heat of hydration. Using the refined evaluation, i.e. including the energy compensation, the heat of hydration curves become approximately equal for TSA A and B. This shows that it is important to consider energies stored within the TSA materials, and that general recommendations concerning low cooling factors may result in too low heat of hydration using TSAs that are evaluated with the traditional method.

In order to investigate effects of the correction factor for our two mixes, the evaluated parameters were applied in 2D structural simulations. Five concrete walls of different thicknesses were used. The results show that temperatures are almost underestimated by 5°C for an “ordinary” cement, and 2°C for a “moderate heat” cement. The consequences for calculated strength development are that the lower strength causes longer hardening time than needed, which might be regarded as being “on the safe side”, but this “extra margin” might not be wanted in practice. For crack risks, the calculated strain/stress ratios are underestimated with at most 0,32 (ordinary cement) and 0,14 (moderate heat cement). A rather common strain/stress ratio in design is 0,70, and based on that the “true” strain/stress ratio might be 1,02 and 0,84, respectively. For the true situation these underestimated temperatures may result in an obvious risk of cracking or at least a significant reduced safety factor. This confirms that it is important to consider energies stored within the TSA materials.

ACKNOWLEDGEMENTS

The authors of the paper acknowledge The Swedish Research Council Formas, Cementa AB and Betongindustri AB. The laboratory tests have been performed in cooperation with personnel from Complab at Luleå University of Technology, which is hereby acknowledged.

REFERENCES

1. Kjellsen, K.O., Detwiler, R.J., and Gjørv, O.E., “Pore Structure of Plain Cement Pastes Hydrated at Different Temperatures,” *Cement and Concrete Research*, Vol. 20, No. 6, November 1990, pp. 927-933.
2. Kjellsen, K.O., Detwiler, R.J., and Gjørv, O.E., “Development of Microstructures in Plain Cement Pastes Hydrated at Different Temperatures,” *Cement and Concrete Research*, Vol. 21, No. 1, January 1991, pp. 179-189.
3. Fjellström, P., Jonasson, J-E., Emborg, M., and Hedlund, H., “Model for Concrete Strength Development Including Strength Reduction at Elevated Temperatures,” *Nordic Concrete Research*, Vol. 45, No. 1, June 2012, pp. 25-44.
4. Concrete: “Heat Development,” Nordtest Method, NT BUILD 388, 1992, 4 pp.

5. RILEM Technical Committee 119-TCE, “Adiabatic and Semi-Adiabatic Calorimetry to Determine the temperature Increase in Concrete due to Hydration Heat of Cement,” RILEM Report 15, Prevention of Thermal Cracking in Concrete at Early Ages, Edited by R. Springenshmid, E & FN Spon, London, 1998, pp. 315-330.
6. Ng, P.L., Ng, I.Y.T., and Kwan, K.H., “Heat Loss Compensation in Semi-Adiabatic Curing Test of Concrete,” *ACI Materials Journal*, Vol. 105, No. 1, January-February 2008, pp. 52-61.
7. Concrete: “Heat Development,” NordTest Method, NT BUILD 488, 1997, 6 pp.
8. Poole, J.L., Riding, K.A., Folliard, K.J., Juenger, M.C.G., and Schindler, A.K., “Hydration Study of Cementitious Materials using Semi-Adiabatic Calorimetry,” *ACI Special Publication* 241CD Concrete Heat Development: Monitoring, Prediction & Management, Edited by K. Wang & A. Schindler, paper SP-241-5, Vol. 241, April 1 2007, pp. 59-76.
9. Riding, K.A., Poole, J.L., Juenger, M.C.G., Schindler, A.K., and Folliard, K.J., “Calorimetry Performed On-Site: Methods and Uses,” *ACI Special Publication* 241CD Concrete Heat Development: Monitoring, Prediction & Management, Edited by K. Wang & A. Schindler, paper SP-241-3, Vol. 241, April 1 2007, pp. 25-38.
10. EN 196-9:2010, ”Methods of Testing Cement – Part 9: Heat of Hydration – Semi-Adiabatic Method,” European Committee for Standardization (CEN), 2010, Brussels.
11. Rastrup, E., “Heat of Hydration in Concrete,” *Magazine of Concrete Research*, Vol. 6, No. 17, September 1954, pp. 79-92.
12. Helland, S., “Norwegian Standards on activation energy and heat release,” IPACS report no. BE96-3843/2001:24-9, TU Luleå, Sweden, 2001, 27 pp.
13. NS 3657:1993, “Concrete Testing – Determination of Heat Release,” Norwegian Standard, September 1993.
14. Whiting, D., Litvin, A., and Goodwin, S.E., “Specific Heat of Selected Concretes,” *Journal of the American Concrete Institute*, Vol. 75, No. 7, July 1 1978, pp. 299-305.
15. Jonasson, J-E., “Slipform Construction – Calculations for Assessing Protection Against Early Freezing,” Swedish Cement and Concrete Research Institute Report, no. 4:84, 1984, Stockholm, 70 pp.
16. Jonasson, J-E., “Modelling of Temperature, Moisture and Stresses in Young Concrete,” Doctoral thesis 1994:153D, Luleå University of Technology, Luleå 1994, 225 pp.
17. Danielsson, U., “Conduction Calorimeter Studies of the Heat of Hydration of a Portland Cement,” Swedish Cement and Concrete Research Institute Report, no. 38, 1966, Stockholm, 121 p. Cited from [19].
18. Byfors, J., Plain Concrete at Early Ages,” Swedish Cement and Concrete Research Institute Report, no. 3:80, 1980, Stockholm, 464 pp.
19. Freiesleben Hansen, P., and Erik, J.P., “Curing of Concrete Structures,” Danish Concrete and Structural Research Institute, Report prepared for CEM – General Task Group No. 20, Durability and Service Life of Concrete structures, December 1984, pp. 45.
20. ConTeSt Pro, “Användarhandbok – ConTeSt Pro (Users manual – Program for Temperature and Stress Calculations in Concrete),” Developed by JEJMS Concrete AB in co-operation with Luleå University of Technology, Cementa AB and Peab Öst AB, Danderyd, Sweden: Cementa AB, pp. 207. (In Swedish).
21. Larson, M., “Estimation of Crack Risk in Early Age Concrete: Simplified Methods for Practical Use,” Licentiate thesis 2000:10, Luleå University of Technology, Luleå 2000, pp. 156.
22. Jonasson, J-E., Wallin, K., Emborg, M., Gram, A., Saleh, I., Nilsson, M., Larson, M., and Hedlund, H., “Temperature Cracks in Concrete Structures: Handbook with Diagrams for Crack Risk Estimation Including Measures for Typical Cases. Part D,” Technical report 2001:14, Luleå University of Technology, Luleå 2001, pp. 107. (In Swedish)